



**Alcamines as Corrosion Inhibitors for Reinforced Steel and  
Their Effect on Cement Based Materials and Mortar  
Performance**

Journal:	<i>RSC Advances</i>
Manuscript ID:	RA-ART-01-2015-000717.R2
Article Type:	Paper
Date Submitted by the Author:	06-Apr-2015
Complete List of Authors:	abdelaziz, Hasan; Faculty of Science, El -Mansoura University, Chemistry Department; El Arish Cement Company, Fouda, abd El-aziz; Faculty of Science, El -Mansoura University, Chemistry Department shalabi, kamal; Faculty of Science, El -Mansoura University, Chemistry Department Elewady, G.Y.; Faculty of Science, El -Mansoura University, Chemistry Department

# Alcamines as Corrosion Inhibitors for Reinforced Steel and Their Effect on Cement Based Materials and Mortar Performance

A.S. Fouda<sup>a</sup>, G. Y Elewady<sup>a</sup>, K .Shalabi<sup>a</sup> and H.K. Abd El-Aziz<sup>a, b</sup>.

<sup>a</sup>Chemistry Department, Faculty of Science, El-Mansoura University, El-Mansoura-35516, Egypt .E-mail: [asfouda@mans.edu.eg](mailto:asfouda@mans.edu.eg).

<sup>b</sup>Chemist, El Arish Cement Co., ArCC, Egypt. E-mail: [has407cem@gmail.com](mailto:has407cem@gmail.com).

## Abstract

Testing steel in solution has the advantage of avoiding the long time necessary for chlorides to penetrate the concrete cover. The effect of some alcamines, namely TIPA85 and CA92 as corrosion inhibitors for reinforced steel bars in 3.5% NaCl and chloride contaminated saturated concrete pore solution (3.5%NaCl+SCP) were discussed with electrochemical techniques. The characteristic effect of studied compounds on the cement and its mortars explained by chemical and physical techniques. Results show that alcamines can be used as corrosion inhibitors, grinding aid raw materials and improver of cement quality. TIPA85 has higher corrosion inhibition efficiency than CA92 as indicated from results of potentiodynamic polarization, electrochemical impedance spectroscopy (EIS), molecular dynamics simulation and quantum chemical calculation methods. Mixed physical and chemical adsorption mechanism is proposed. Adsorption of these alcamines was found to follow the Langmuir's adsorption isotherm.

## Introduction

The reinforcement steel is used in majority of reinforced concreted infrastructures such as buildings and bridges. Many reinforced concrete structures have given excellent service with minimal maintenance. Corrosion of reinforcement steel is a major deterioration mechanism for concrete structures in cold, marine and industrial environments. The corrosion processes are closely relate to the concrete and environmental factors. Several solutions to this problem have been proposed and tested, though to date no ideal solution has been found. Some of these methods involve increasing the concrete cover over the rebar, reducing water/cement ratios, using denser concrete, using latex or polymer modified concrete overlays, adding waterproofing membrane with asphalt overlay, coating the rebar with epoxy or zinc, protecting the rebar cathodically, and using corrosion inhibiting admixtures. Corrosion Inhibitors for reinforced Steel can divided in to admixed inhibitors and surface applied inhibitors. We suggested a new method by adding the corrosion inhibitor as interground additive in cement production to produce cement with more inhibiting character for steel corrosion by aggressive chloride ions.

Alcamines are used as components in corrosion inhibitor blends of usually complex formulations [1]. In addition, alcamines used as cement grinding aids GA by arrange their dipoles so that they saturate the charges on the newly formed particle surface, reducing re-agglomeration. GA has as its ultimate objective decreasing the energy consumption to obtain a given fineness or flow of cement [2, 3]. Quantum chemistry calculation has been widely used to evaluate the inhibition performance of corrosion inhibitors, which can quantitatively study the relationship between inhibition efficiency and molecular reactivity [4–6]. Compared with quantum chemistry method, molecular mechanics can used to study small molecules as well as large molecular systems. Molecular mechanics method would be a better choice for large systems. With molecular mechanics methods, the adsorption state of inhibitor monolayer formed on metal surface can be investigated via analysis of interfacial configuration, interaction between monolayer and metal surface, and cohesive energy of monolayer, etc. [7–8].

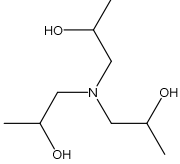
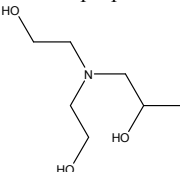
The objective of this work is to study the role of well-known alcamines as corrosion inhibitors on reinforced steel in 3.5% NaCl solution and in contaminated solution of saturated calcium hydroxide  $\text{Ca}(\text{OH})_2$ , that is used as simulated concrete pore (SCP) solution, with 3.5% NaCl [9-12] by potentiodynamic polarization and electrochemical impedance spectroscopy (EIS) methods. We add these materials to cement mills in cement industry to give additional features on cement quality beside their works as cement grinding aids. Finally, we calculate the more relevant molecular properties on its action as corrosion inhibitors by molecular dynamics and quantum chemistry (DFT) to discuss the adsorption configuration, charge distribution and frontier orbital energy.

## Experiments and methods

### Chemicals and materials

Sodium chloride, calcium hydroxide, ethyl alcohol and acetone were purchased from Algamhoria Co., Egypt. Alcamines (TIPA85 & CA92) were supplied from NINGBO LUCKY CHEMICAL INDUSTRY CO., LTD (China). The molecular and structure formula of TIPA85 and CA92 are show in Table 1. Bi-distilled water was use for preparing test solutions for all measurements. The corrosion tests performed on Ezz reinforced steel of Grade B400B-R according to EGYPTIAN STANDARD (ES-262/2000). Clinker, gypsum and limestone obtained from El-Arish cement Company (ArCC). CEN, EN 196-1 Standard sand purchased from S.N.L (Société Nouvelle du Littoral) France.

Table1: Technical Data obtained from NINGBO LUCKY CHEMICAL INDUSTRY CO.,LTD

Type	Product code	Chemical name& Structure	Mol.Wt	Appearance (25°C)	Content
Alcamine	TIPA85	Triisopropanolamine 	191.15	Colorless liquid	≥85
	CA92	Diethanolisopropanolamine 	163.21	Colorless liquid	≥92

### Electrochemical measurements

Two electrochemical techniques, namely potentiodynamic polarization and electrochemical impedance spectroscopy (EIS) were been used for study the corrosion behavior. All experiments were conduct in a conventional three electrodes glass cell. A Pt electrode used as counter electrode and a saturated calomel electrode (SCE) used as reference electrode in this study. The deformed reinforced steel bar (as working electrode) cut into 15.0 cm with two ends and changed by reamer to plain reinforced steel. Plain reinforced steel sealed with epoxy resin leaving a working area of 0.384 cm<sup>2</sup> and copper wire was connect at other end of the rod. The working electrode were polished with 80, 220, 400, 600, 1000, 1200 grades of emery paper polishing paper. After being polished they were rinse by acetone and ethanol, dried, and wrapped in filter paper. The polished samples were been kept in a hot oven to keep them dry. The experiments carried out in 3.5%NaCl solution after 30 minutes of immersion of working electrode at temperature (20°C±1°C) and the open circuit potential (OCP) was note. The experiments were been also carried out in simulated concrete pore (SCP) solution contaminated with 3.5% NaCl at temperature (20°C±1°C) after 60 minutes immersion and the open circuit potential (OCP) was noted.

Potentiodynamic polarization experiments carried out using a Gamry Instrument Series G750™ Potentiostat/Galvanostat/ZRA with a Gamry framework system based on ESA400. Gamry applications include DC105™ software for Potentiodynamic measurements.

A computer was been used for collecting data. Echem Analyst 5.5 Software used for plotting, graphing and fitting data. Sweeping the potential by several hundred millivolts -400 to +400 mV at a scan rate 1 mVS<sup>-1</sup> relative to the open circuit potential, E<sub>oc</sub>, draws Tafel Plots. The degree of surface coverage  $\theta$  and inhibition efficiency IE% [13] were been calculated from:

$$\theta = \frac{i_{\text{corr}}^{\circ} - i_{\text{corr}}}{i_{\text{corr}}^{\circ}} \quad (1) \quad , \quad IE_p \% = \frac{i_{\text{corr}}^{\circ} - i_{\text{corr}}}{i_{\text{corr}}^{\circ}} \times 100 \quad (2)$$

where  $i_{\text{corr}}^{\circ}$  and  $i_{\text{corr}}$  are the corrosion current densities of uninhibited and inhibited solution, respectively.

Electrochemical impedance spectroscopy (EIS) experiments carried out using Gamry Instrument Series G750™ Potentiostat/Galvanostat/ZRA with a Gamry framework system based on ESA400. Gamry applications include EIS300 software for EIS measurements. EIS measurements were carried out in a frequency range of 100 kHz to 100 mHz with amplitude of 5mV peak-to-peak using ac signals at respective corrosion potential.

### Chemical and physical techniques

The effects of the corrosion inhibitors in cement production and on cement quality discussed by

Chemical technique: X-Ray fluorescence chemical analysis (XRF)

Physical techniques: Specific Blaine surface measurements, Standard consistency, Initial and Final Setting Times measurements, Compressive and flexural strength measurements

### Chemical techniques (X-Ray fluorescence chemical analysis)

Corrosion inhibitor used as interground additive in cement production (packing of inhibitor on cement granulated) by grinding 5kg of cement raw materials [ blank 1 (95%clinker+5%gypsum), blank 2 (95%clinker+5%gypsum+4%limestone)] in order to produce samples of CEM I-52.5N scale using a lab ball mill with identical grinding time 45minutes. Chemical and mineralogical composition of each cement samples were carried out using ARL 9900 IntelliPower Series X-Ray Spectrometer Instrument according to the European standard EN 196-2 with ARL Thermo OXSAS V.1.4 software. A computer was used for collecting data. Percentages of Silicon dioxide (SiO<sub>2</sub>), Aluminum oxide (Al<sub>2</sub>O<sub>3</sub>), Ferric oxide (Fe<sub>2</sub>O<sub>3</sub>), Calcium oxide (CaO), Magnesium oxide(MgO), Sulfur trioxide (SO<sub>3</sub>), sodium oxide (Na<sub>2</sub>O), Potassium oxide (K<sub>2</sub>O), chloride content (Cl). Free lime and Loss on ignition (LOI) are measured individually. Using chemical compositions, compound compositions C3S, C2S, C3A and C4AF were calculated using Bogue Composition Formulas [14]. From the oxides of different elements, cement moduli i.e. LSF, SM and AM were also calculated.

## Physical techniques

### Specific Blaine surface measurements of cement

Cement fineness is measured as mass surface by observing the time a given of air takes to go through a bed of compacted cement with a specific size and porosity. The S mass surface of the test cement expressed in  $\text{cm}^2/\text{g}$ , in accordance with the European standard EN 196-6. Determination of the specific Blaine surface of cement in accordance with the European standard EN196-6 were carried out using Automatic Blaine device ToniPERM standard. Collecting data was been done from device screen.

### Standard consistency, Initial and Final Setting Times measurements of cement

Standard consistency (see equation 3) determined using the Vicat Apparatus according to European standard EN 196-3 standard for collected samples. Determination of Initial and Final Setting Times of Cements in accordance with the European standard EN 196-3 were be carried out using Automatic Vivat Needle Apparatus ToniSET CLASSIC. A computer was use for collecting data .PRISAL Software was been used for plotting, graphing and fitting data.

$$\text{standard consistency}\% = \frac{\text{Weight of water added}}{\text{Weight of cement}} \times 100 \quad (3)$$

### Compressive and flexural strength measurements of cement

Compressive and flexural strength determinates on prismatic test specimens 40 mm x 40 mm x 160 mm in size. These specimens cast from a batch of plastic mortar containing one part by mass of cement and three parts by mass of standard sand with a water-cement ratio of 0.50. The mortar is prepared by mechanical mixing and is compacted in a mould using a standard jolting apparatus. The specimens in the mould are stored in a moist atmosphere for 24 h and then the demoulded specimens are stored under water until strength testing. Compressive and flexural strength experiments were carried out using Automatic Compression and Bend test Plant **Toni PRAX** testing machines with **ToniTrol**<sup>®</sup> and **testXpert**<sup>®</sup> operation software that developed by **Zwick** company. A computer was use for collecting data .**Zwick testXpert**<sup>®</sup> Software was use for plotting, graphing and fitting data. Remove the specimens from the water not more than 15 min before the test carried out. Cover the specimens with a damp cloth until tested.

### Molecular mechanics and dynamics methods

Molecular dynamics (MD) is a computer simulation of physical movements of atoms and molecules in the context of N-body simulation. The atoms and molecules are been allowed to interact for a certain time, giving a view of the motion of the atoms. The forces between the particles and potential energy are define by molecular mechanics force fields. Molecular dynamic simulation studies were been performed to simulate the adsorption structure of the studied compounds and press on the understanding of interactions between these compounds and iron surface. The adsorption progress of these compounds on iron surface [15] Fe (1 1 0) is simulated by performing molecular dynamics (MD) using Discover molecular dynamics module in Materials Studio version 6.0 software (available from Accelrys Inc., San Diego, CA).The whole system was simulated in water. The simulation of the interaction between the involved molecules and the Fe (1 1 0) surface was carried out in a simulation box (32.27 x 32.27 x 49.97 Å<sup>3</sup>) with periodic boundary conditions in order to simulate a representative part of an interface devoid of any arbitrary boundary effects . The temperature was fixed at 298 K, with the NVT ensemble, with a time step of 1.0 fs and simulation time of 30.0 ps. The system was quenched every 5000 steps with the Fe (1 1 0) surface atoms constrained. The interaction energy  $E_{\text{Fe-inhibitor}}$  of the Fe surface with the inhibitor was calculated according to the following equation [16]:

$$E_{\text{Fe-inhibitor}} = E_{\text{complex}} - (E_{\text{Fe}} + E_{\text{inhibitor}}) \quad (4)$$

where :  $E_{\text{complex}}$  is the total energy of the Fe crystal together with the adsorbed inhibitor molecule,  $E_{\text{Fe}}$  and  $E_{\text{inhibitor}}$  are the total energy of the Fe crystal and free inhibitor molecular, respectively. In addition,  $E_{\text{binding}}$  is the binding energy was the negative value of the interaction energy  $E_{\text{Fe-inhibitor}}$ .

### Quantum chemical calculation

$E_{\text{HOMO}}$ (highest occupied molecular orbital energy),  $E_{\text{LUMO}}$  (lowest unoccupied molecular orbital energy) and Fukui indices calculations were performed using DMol<sup>3</sup> module in Materials Studio version 6.0 [17,18]. These calculations employed an ab initio, gradient-corrected functional (GGA) method with a double numeric plus polarization (DNP) basis set and a Becke One Parameter (BOP) functional. It is well-known that the phenomena of electrochemical corrosion appear in aqueous phase. DMol<sup>3</sup> includes certain COSMO<sup>1</sup> [19] controls, which allow for the treatment of solvation effects.

## Results and discussion

### Electrochemical measurements

#### Potentiodynamic polarization measurements

Reinforced steel is not completely passive when put in an electrolytic solution. Chloride ion is more reactive to make corrosion than formation of passive film. In our study, there are two regions. First one related to active corrosion that occurred by chloride ions and the other related to small oxide film (passive film) due to oxygen found in solution that is more stabilized by inhibitors existence. The values of

pitting potentials depends on the concentrations of inhibitive compounds and aggressive anions (which break down the oxide film) in the solution.

Figure 1 depict polarization curves for the reinforced steel electrode after 30 minutes of immersion reinforced steel in 3.5% NaCl (blank1) with different concentrations of TIPA85. Similar curves were obtain for CA92 (not shown). Compared with the control solution, it was evident that the increase of compounds concentration would result in a decrease of corrosion current density and an increase of passive range and inhibition efficiency (i.e., the inhibition efficiency was more pronounced with the increase of alcamines content). This suggested that a more and more complete and stable barrier film was forming on the steel surface.

Tables 2 give the fitted electrochemical from the polarization curve.  $E_{corr}$ ,  $E_{pit}$  were corrosion potential and pitting potential, respectively.  $E_{pit}-E_{corr}$  was the width of the passive range, calculated from the difference between  $E_{pit}$  and  $E_{corr}$ .

Both cathodic Tafel slopes ( $\beta_c$ ) and anodic Tafel slopes ( $\beta_a$ ) do not change remarkably, which indicates that the mechanism of the corrosion reaction does not change and the corrosion reaction is inhibited by simple adsorption mode [20]. The irregular trends of  $\beta_a$  and  $\beta_c$  values indicate the involvement of more than one type of species adsorbed on the metal surface. The inhibition efficiency [21] (IE %) calculated by the equation (2) and indicated that TIPA85 has higher inhibition efficiency than CA92.

Figure 2 observed polarization curves for reinforced steel electrode after 60 minutes of immersion in aqueous solutions of SCP contaminated with 3.5% sodium chloride (blank2) in the absence and presence of 150-ppm of alcamines. We take in consideration that this concentration has the highest inhibition efficiency for our studied compounds as indicated in pervious section. Table 2 gives the fitted electrochemical data from the polarization curve. The results indicated that TIPA85 has higher inhibition efficiency than CA92.

The mixed inhibitors that act both as anodic and cathodic reaction suppressants, it is evident that the presence of these compounds retard both the metal dissolution and the cathodic process without causing significant change in corrosion potential ( $E_{corr}$ ). Inspection of figures 1, 2 reveals that  $E_{corr}$  values in the presence of inhibitors have no definite shift, suggest that they are mixed type inhibitors [22].

Generally, the increase of the inhibitors concentration shifts the corrosion potential into a less negative direction in figure 1, what can explained by a small domination of the anodic reaction inhibition. Vice versa in figure2, inhibitors concentration shifts the corrosion potential into a more negative direction what can explained by a small domination of the cathodic reaction inhibition.

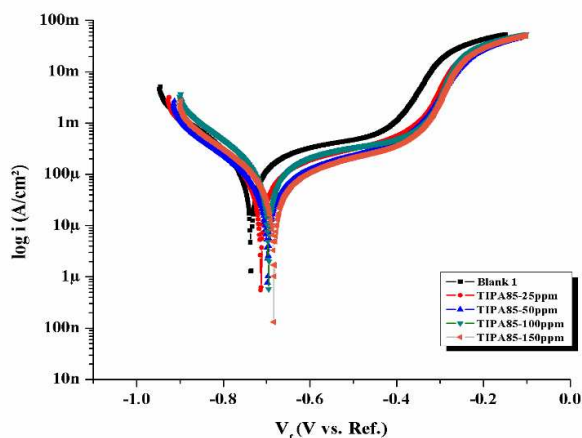


Fig.1 Potentiodynamic polarization plots for corrosion of reinforced steel in 3.5% NaCl in absence and presence of different concentrations of TIPA85 at  $20^{\circ}\text{C}\pm 1^{\circ}\text{C}$

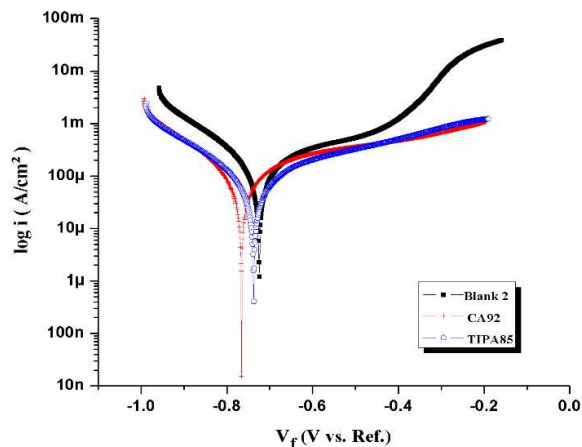


Fig. 2: Potentiodynamic polarization plots for corrosion of reinforced steel in SCP + 3.5%NaCl in absence and presence of 150 ppm of alcamines at  $20^{\circ}\text{C}\pm 1^{\circ}\text{C}$ .

Table 2: The electrochemical parameters obtained for reinforced steel in 3.5% NaCl solution in absence and presence of different concentrations of alcamines and that obtained for reinforced steel in 3.5% NaCl+SCP solution in absence and presence of 150ppm of alcamines at 20°C±1°C.

COMP.,	Conc., ppm	-E <sub>Corr</sub> (mV/SCE)	-E <sub>pit</sub> (mV/SCE)	E <sub>pit</sub> -E <sub>corr</sub> (mV/SCE)	i <sub>corr</sub> (µA/cm <sup>2</sup> )	β <sub>a</sub> (mV/dec)	β <sub>c</sub> (mV/dec)	Θ	IE%	CR., Mpy
Blank 1	---	736.0	360.8	375.2	93.5	158.3	100.4	-	-	42.74
TIPA85	25	713.0	309.7	403.1	26.8	69.3	61.4	0.713	71.3	11.04
	50	698.0	286.8	411.2	21.0	51.2	45.8	0.775	77.5	8.85
	100	696.0	287.8	408.2	19.5	56.2	51.4	0.791	79.1	8.92
	150	683.0	289.9	393.1	16.6	54.7	48.7	0.823	82.3	7.59
CA92	25	713.0	311.8	401.2	47.1	134.6	94.8	0.496	49.6	21.54
	50	709.0	303.4	405.6	34.0	92.3	75.8	0.636	63.6	15.56
	100	707.0	301.1	405.9	23.8	68.7	55.4	0.746	74.6	10.86
	150	691.0	285.7	405.3	22.7	52.7	45.1	0.757	75.7	10.35
Blank 2	-----	724.1	-----	-----	38.3	72.0	53.8	-----	-----	17.50
TIPA85	150	737.0	-----	-----	13.8	48.9	47.5	0.639	63.9	6.09
CA92	150	765.8	-----	-----	16.2	48.8	45.4	0.577	57.7	7.41

### Electrochemical impedance spectroscopy

EIS is a widely applied electrochemical technique for studying the corrosion performance of steel in both reinforced concrete and in simulated pore solution [23-26]. Nyquist and Bode plots obtained for the reinforced-steel electrode at respective corrosion potentials after 30 minutes of immersion in 3.5%NaCl in presence and absence of various concentrations of TIPA85 are show in Figure 3. The experimental EIS response was been fitted using an equivalent circuit, consisting of two time constants in series with the electrolyte resistance. The corresponding equivalent circuit [27] was been shown in Figure 4. The fitted results of the experiment data by the proposed equivalent circuit are in Table 3. The results indicate that the values of  $R_{ct}$  and  $R_f$  increase with content of inhibitors. That is due to the growing adsorption film. The increase in  $R_{ct}$  suggests that the amount of inhibitor molecules adsorbed on the reinforced steel surface increases and consequently results in the decreasing of active sites where dissolution of iron is easy. This barrier can effectively prevent chloride ion and oxygen close to the metal surface, and thereby inhibit pitting corrosion. The most pronounced effect and the highest  $R_{ct}$  were been obtained by TIPA85 at all concentrations. The high  $R_{ct}$  values are generally associated with slower corroding system [28, 29].The meaning of the symbols shown in Figure 4 and in Table 3 were as follows:

$R_s$  = solution resistance  $R_{ct}$  = charge transfer resistance,  $R_f$  = film resistance,  $CPE_1$ = constant phase elements to replace the film capacitance ( $C_f$ ),  $CPE_2$ = constant phase elements to replace the electric double layer ( $C_{dl}$ )

The presence of the CPE is due to the distributed surface heterogeneity, roughness, fractal geometry, electrode porosity, and due to current and potential distributions related with electrode geometry [30, 31]. The inhibition efficiency (IE %) calculated by the equation (5) listed in Table 4 and indicated that: TIPA85 has higher inhibition efficiency than CA92.

$$IE\% = \frac{R_{ct} - R_{ct}^*}{R_{ct}} \times 100 \quad (5)$$

where  $R_{ct}$  and  $R_{ct}^*$  are the charge-transfer resistances with and without the inhibitors, respectively

Figure 5 Characterize EIS curves for reinforced steel electrode in aqueous solutions of SCP contaminated with 3.5% NaCl in the absence and presence of alcamines with concentration 150-ppm after 60 minutes of immersion. Table 3 gives the fitted electrochemical from the EIS curves. TIPA85 has higher inhibition efficiency than CA92 as shown in Table 3.

The difference of inhibition efficiency from the two methods may attributed to the different surface status of the electrode in the two measurements. EIS were performed at the rest potential, while in polarization measurements the electrode potential was polarized to high over potential, non-uniform current distributions, resulted from cell geometry, solution conductivity, counter and reference electrode placement, etc., will lead to the difference between the electrode area actually undergoing polarization and the total area [32].

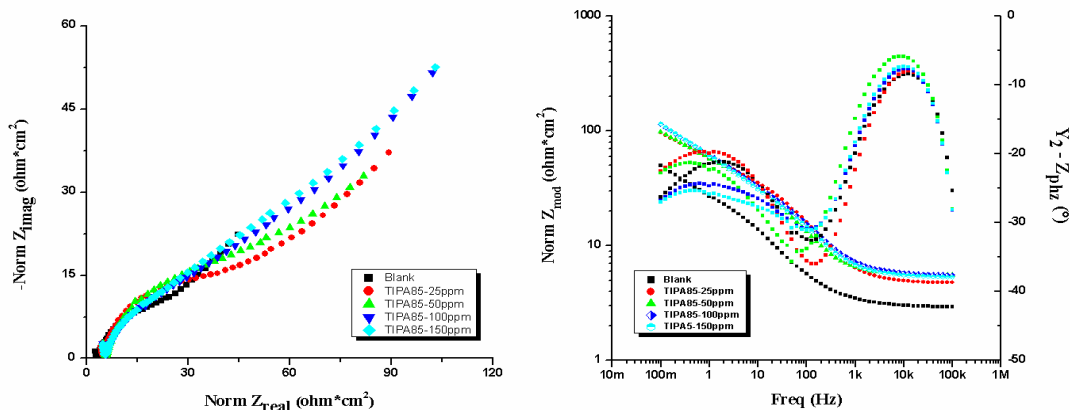


Fig.3: Potentiostatic EIS Nyquist and Bode plots for reinforced steel in 3.5%NaCl in the absence and presence of TIPA85 at 20°C±1°C.

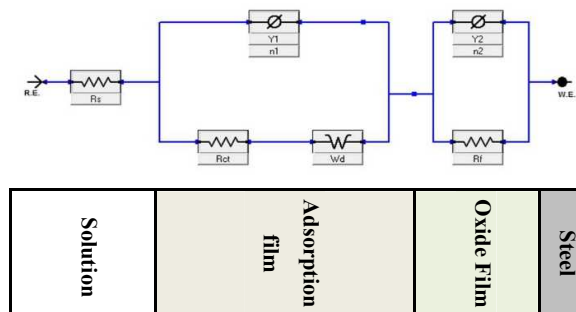


Fig.4: Electrochemical equivalent circuit used to fit the impedance spectra

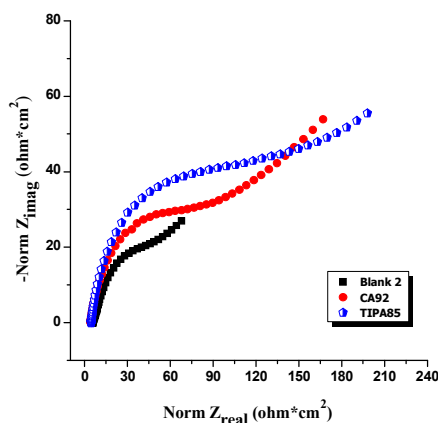


Fig.5: Potentiostatic EIS Nyquist plots for corrosion of reinforced steel in 3.5%NaCl + SCP in absence and presence of 150ppm of alcamines at 20°C±1°C.

Table 3: EIS parameters obtained for reinforced steel in 3.5% NaCl solution in absence and presence of different concentrations of alcamines and that obtained for reinforced steel in 3.5% NaCl+SCP solution in absence and presence of 150ppm of alcamines at 20°C±1°C.

COMP.,	Conc., ppm	R <sub>s</sub> Ωcm <sup>2</sup>	CPE <sub>1</sub>		R <sub>CT</sub> Ωcm <sup>2</sup>	CPE <sub>2</sub>		R <sub>F</sub> Ωcm <sup>2</sup>	W mΩ <sup>-1</sup> s <sup>n</sup> cm <sup>-2</sup>	IE%
			Y <sub>1</sub> , μΩ <sup>-1</sup> s <sup>n</sup> cm <sup>-2</sup> x10 <sup>3</sup>	n <sub>1</sub>		Y <sub>2</sub> μΩ <sup>-1</sup> s <sup>n</sup> cm <sup>-2</sup> x10 <sup>3</sup>	n <sub>2</sub>			
Blank 1	---	2.44	1.77	0.60	24.14	1.09	0.94	2.41	5.37	---
TIPA85	25	4.39	2.10	0.62	48.57	0.97	0.99	2.93	3.20	50.3
	50	5.19	0.68	0.64	53.53	0.46	0.91	3.26	2.43	54.9
	100	4.97	0.63	0.56	59.17	0.41	0.92	4.45	2.24	59.2
	150	4.73	0.46	0.55	78.49	0.30	0.86	5.42	2.15	69.2
CA92	25	4.57	0.66	0.62	40.47	0.58	0.88	2.66	4.30	40.4
	50	4.86	0.65	0.63	48.38	0.47	0.99	2.95	3.04	50.1
	100	4.48	0.63	0.59	54.49	0.28	0.97	3.31	2.98	55.7
	150	4.80	0.48	0.58	64.32	0.25	0.93	3.44	2.96	62.5
Blank 2	-----	5.60	0.55	0.73	49.57	0.34	0.78	1.48	5.92	-----
CA92	150	4.17	0.13	0.66	121.42	0.02	0.94	30.04	2.22	59.2
TIPA85	150	4.62	0.12	0.71	142.38	0.02	0.92	31.40	2.28	65.2

### Adsorption isotherm

Adsorption isotherm was particularly important in understanding the interaction mechanism between organic molecules and metal surface. Several adsorption isotherms were assessed and the Langmuir adsorption isotherm found to be the best description of the adsorption behavior of alcamines. The regression coefficient  $R^2 = 0.999$  suggest a good relation between  $C/\theta$  and  $C$ . In the present investigation, the data obtained from polarization measurements fitted well with Langmuir isotherm, as shown in Figure 6. The degree of surface coverage  $\theta$  for different concentrations of the inhibitors in 3.5%NaCl has evaluated from polarization measurements using equation (1). All the calculated thermodynamic parameters were list in Table 4. According to Langmuir isotherm, the degree of surface coverage was related to inhibitor concentration as [33-35]:

$$\frac{C_{inh}}{\theta} = \frac{1}{K} + C_{inh} \quad (6)$$

where :  $C_{inh}$  is the inhibitor concentration,  $\theta$  is the fraction of the surface coverage,  $K$  is the modified adsorption equilibrium constant which can be related to the free energy of adsorption  $\Delta G_{ads}^{\circ}$  and  $C_{solvent}$  is the molar concentration of solvent which in the case of the water is  $55.5 \text{ mol L}^{-1}$  by the following equation:

$$K_{ads} = \frac{1}{C_{solvent}} \exp\left(\frac{-\Delta G_{ads}^{\circ}}{RT}\right) \quad (7)$$

The  $K_{ads}$  values in Table 4 could take as a measure of the strength of the adsorption forces between the inhibitor molecules and the metal surface. The higher value of  $K_{ads}$  revealed that the inhibitor performed stronger adsorption ability onto the steel surface. Therefore, TIP485 has strong adsorption than CA92.  $\Delta G_{ads}^{\circ}$  value was an expression of adsorption character. As reported, value of  $\Delta G_{ads}^{\circ}$  up to  $-20 \text{ kJ/mol}$  indicated a physical adsorption, while that of more negative than  $-40 \text{ kJ/mol}$  involved sharing or transferring of electrons from the inhibitor molecules to the metal surface to form a coordinate type bond (chemical adsorption) [36]. The magnitudes of  $\Delta G_{ads}^{\circ}$  of the investigated compounds shows that a comprehensive adsorption (physical and chemical adsorption) might be occur [37].

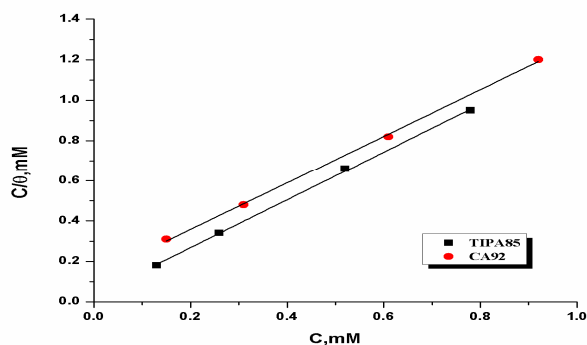


Fig.6: Langmuir adsorption plots for reinforced-steel in 3.5%NaCl containing various concentrations of alcamines at  $20^{\circ}\text{C}\pm 1^{\circ}\text{C}$ .

Table 4: Thermodynamic parameters for the adsorption of alcamines on steel in 3.5%NaCl at  $20^{\circ}\text{C}\pm 1^{\circ}\text{C}$ .

Langmuir Adsorption isotherm					
Inhibitor	slope	Log K	$K \times 10^{-3}, \text{M}$	$-\Delta G_{ads}^{\circ}$ $\text{kJ} \cdot \text{mol}^{-1}$	$R^2$
TIP485	1.1	4.51	32.36	35.1	0.999
CA92	1.1	3.89	7.76	31.6	0.999

### Chemical and physical techniques

The influence of corrosion inhibitors on cement based materials and mortar performance was observed by chemical and physical techniques.

#### Chemical techniques (X-Ray fluorescence chemical analysis)

Data in Table 5 shows sulphate, loss on ignition, chlorides, moduli and mineralogical composition of cement (blank 1 and blank 2) that grinding in a lab ball mill with and without the addition of compounds. The results indicated that cement have nearly optimized  $\text{SO}_3$  and nearly identical C3S. This leads to make a good study of the effect of inhibitors on cement based materials and mortar performance including Blaine, setting time, and cement strength.

#### Physical techniques

##### Specific Blaine surface of cement

The results in Table 5 indicated that Blaine surface of cements increase with the addition of studied compounds that supposed the used of these compounds as raw materials for cement grinding aids [38].



Table 5: Analysis of cement (95%Clinker + 5%Gypsum) and cement (95%Clinker + 5%Gypsum + 4%Limestone)

Comp.,	Conc., ppm	SO <sub>3</sub>	LOI	FL	Blaine Cm <sup>2</sup> /g	Cement moduli			Mineralogical composition			
						LSF	SM	AM	C3S	C2S	C3A	C4AF
Blank I	----	2.85	0.83	0.68	3317	93.44	2.10	1.39	51.14	20.01	8.09	12.37
TIPA85	150	2.81	0.85	0.62	3366	92.84	2.11	1.38	50.50	21.21	8.08	12.49
CA92	150	2.88	0.85	0.55	3358	94.02	2.11	1.38	53.52	18.42	8.01	12.43
Blank II	----	2.89	2.30	0.80	3570	97.69	2.08	1.38	59.62	11.38	7.80	12.04
TIPA85	150	2.90	2.35	0.67	3615	97.49	2.08	1.38	59.70	11.41	7.85	12.10
CA92	150	3.15	2.43	0.69	3625	96.54	2.11	1.51	56.51	13.7	8.55	11.31

### Standard consistency, Initial and Final Setting Times of cement

The results of Standard consistency, Initial and Final Setting times of cement pastes depict in Table 6. The Standard consistency results of cement packed with inhibitors have a slightly difference from cement without inhibitor which indicated the compatibility of cement and admixtures [39]. In addition, the results indicated that the inhibitors affects both Initial and Final Setting Times of cements [38].

Table 6: The results of Standard consistency, Initial and Final Setting times of cement pastes.

Cement-based materials				
	Conc., ppm	Setting Time (min)		Water consistency (%)
		Initial	Final	
Blank I	-	115	145	27.4
TIPA85	150	125	150	27.0
CA92	150	145	170	28.2
Blank II	-	125	155	28.0
TIPA85	150	135	160	27.4
CA92	150	125	155	27.4

### Flexural and Compressive strength of Cement

The results of Flexural and Compressive strength of cement mortars for 2 days and 28 days according to EN-197-1 before and after addition of alcamines in lab mill depict in Table 7. The results indicated that cement with 150 ppm alcamine have good effects on Flexural and Compressive strength of cement. In addition, the inhibitors enhanced the Flexural and Compressive strength of cement (95%Clinker +5%Gypsum+4%Limestone) packed with inhibitors higher than that of cement (95%Clinker +5%Gypsum) packed with same inhibitors. Limestone used in cement industry as cement additive to decrease the cost of industrial process and environmental pollution. A good way for limiting the negative effect of clinker reduction on strength is the use of cement grinding aids. Besides the positive effect on grinding (increase in mill output and / or fineness), there is a positive effect on clinker reactivity [40]. We take the effect of these materials on increment of 28 days strength under industrial tap water as supported for anti-corrosive behavior from the relation between cement strength and porosity. The increment of strength [41] means decreasing the porosity thus the amount of chloride that ingress through concretes pores decreased, therefore the corrosion inhibition of rebar steel enhanced.

Table 7: The results of Flexural and Compressive strength of cement mortars for 2 days and 28 days according to EN-197-1

Cement-based materials					
Comp.,	Conc., ppm	Cement strength (2 days)		Cement strength (28 days)	
		Flexural (N/mm <sup>2</sup> )	Compressive (N/mm <sup>2</sup> )	Flexural (N/mm <sup>2</sup> )	Compressive (N/mm <sup>2</sup> )
Blank I	-----	5.4	29.0	7.5	57.9
TIPA85	150	5.3	27.4	8.1	63.8
CA92	150	5.4	30.1	7.5	59.0
Blank II	-----	5.1	26.1	8.4	55.8
TIPA85	150	5.2	30.2	8.6	63.2
CA92	150	5.8	33.7	8.8	63.5

### Molecular mechanics and dynamics methods

The MD simulation was performed to study the adsorption behavior of the two inhibitors on the Fe (110) surface. The system reaches equilibrium only if both of the temperature and energy reach balance (see Figure 7). Figure 8 shows the system that simulated in a water solution. According to the equilibrium configuration of the two inhibitor adsorbed on Fe (110) surface, we can draw a conclusion that both alcamines can be adsorbed on the Fe surface mainly through the heteroatoms. In this way, the exposed part of Fe surface can be reduced by alcamines covering, consequently preventing the surface from the water. Therefore, the corrosion inhibition is achieved by this factor. It can be inferred that the inhibitor molecules will form a waterproof film on the Fe surface after being added to the solution. The value of the interaction and binding energy of the two inhibitors on Fe (110) surface are listed in Table 8. All binding energies in Table 8 are positive, showing that the combination processes of corrosion inhibitors with iron crystal are exothermic. As the value of the binding energy increases, the more easily the inhibitor adsorbs on the metal surface, the higher the inhibition [42]. TIP A85 has a greater binding energy than that of CA92, reflecting the higher stability of the formed complex and accordingly increasing its inhibition efficiency. Thus, TIP A85 has a greater inhibitor efficiency and this is consistent with experimental results.

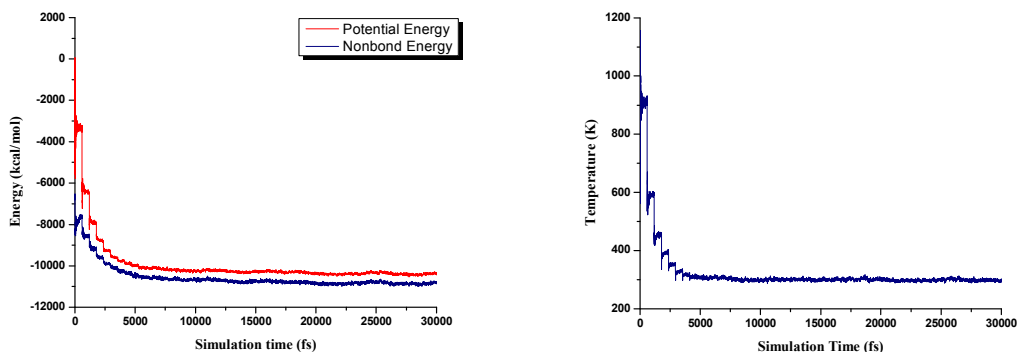


Fig. 7: Energy and Temperature fluctuation curves of the TIP A85- MD simulation

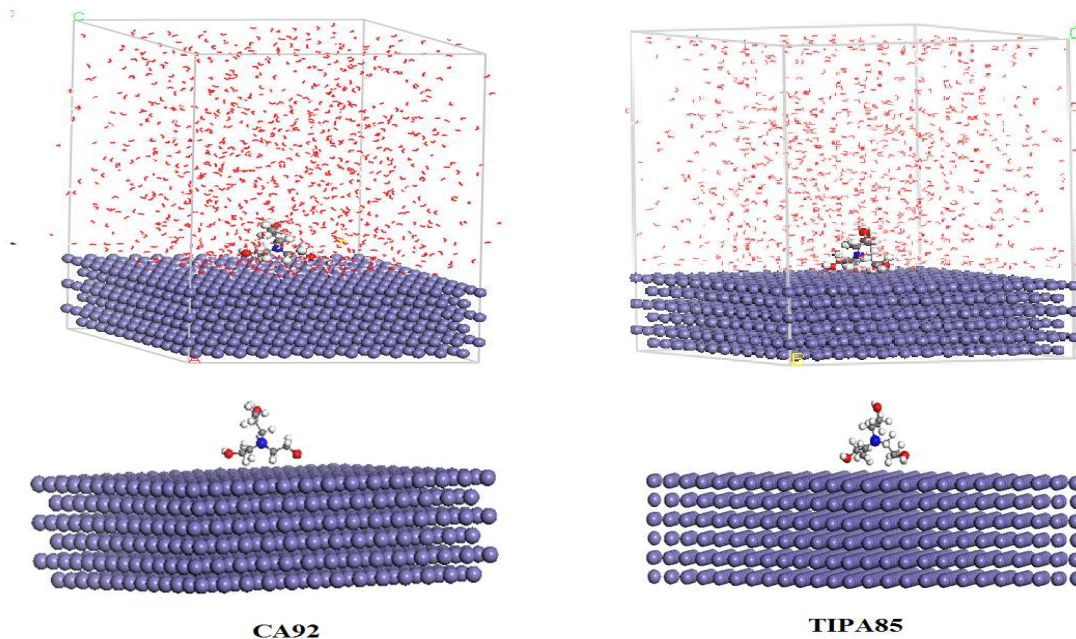


Fig. 8: Equilibrium adsorption configurations of alcamines on Fe (110) surfaces obtained by molecular dynamics simulations.

Table 8: Interaction and binding energy of the two inhibitors on Fe (1 1 0) surface

Inhibitor	$E_{\text{Fe-inhibitor}}$ (kJ/mol)	$E_{\text{binding}}$ (kJ/mol)
TIP A85	-246.4	246.4
CA92	-127.1	127.1

### Quantum chemistry calculation

For establishing the active site of the inhibitor molecule, three influence factors: natural atomic charge, distribution of frontier molecular orbital and Fukui indices are considered. According to classical chemical theory, all chemical interactions are by either electrostatic or orbital. Electrical charges in the molecule were obviously the driving force of electrostatic interactions. It has been proven that local electron densities or charges are important in many chemical reactions and physicochemical properties of compound [43]. Pearson introduced the quantities of electronic hardness ( $\eta$ ) and softness ( $s$ ) in his hard-soft-acid-base principle [44] (HSAB) in the early stage of the reactivity theory. The relationship between hardness or softness and the chemical reactivity was given through the HSAB principle. The optimized structure, HOMO and LUMO shapes obtained by DMol<sup>3</sup> module are shown in Figure 9, which more concentrated on heteroatoms. Table 9 shows the quantum chemical calculation parameters obtained by DFT method. These parameters are mainly ionization potential ( $I_p$ ), electron affinity ( $E_A$ ), energy gap ( $\Delta E$ ), global hardness ( $\eta$ ), softness ( $s$ ), chemical potential (CP) and total energy ( $E_{tot}$ ). The concepts of electronegativity ( $\chi$ ), global hardness ( $\eta$ ) [45], softness ( $\sigma$ ) and chemical potential (CP), were calculated in terms of  $I$  and  $E_A$  [46,47] from the following equations:

$$\eta = \frac{I_p - E_A}{2} \quad (8), \quad \sigma = \frac{1}{\eta} = \frac{2}{I_p - E_A} \quad (9), \quad \chi = -CP = \frac{I_p + E_A}{2} \quad (10)$$

The global electrophilicity index ( $\omega$ ) that introduced by Parr [48], the fraction of electrons transferred  $\Delta N$  from the inhibitor to metallic surface [49] and the energy of back donation  $\Delta E_{back-donation}$  were calculated in terms global hardness ( $\eta$ ) and electronegativity ( $\chi$ ) from the following equations:

$$\omega = \frac{\chi^2}{2\eta_{inh}} \quad (10), \quad \Delta N = \frac{\chi_{Fe} - \chi_{inh}}{2(\eta_{Fe} + \eta_{inh})} \quad (11), \quad \Delta E_{back-donation} = -\frac{\eta_{inh}}{4} \quad (12)$$

Where  $\chi_{Fe}$  and  $\chi_{inh}$  denote the absolute electronegativity of iron and inhibitor molecule, respectively.  $\eta_{Fe}$  and  $\eta_{inh}$  denote the absolute hardness of iron and the inhibitor molecule, respectively. In order to calculate the fraction of electrons transferred, a theoretical value of  $\chi_{Fe} = 7.0$  eV [48] and  $\eta_{Fe} = 0$  by assuming that for a metallic bulk  $I = A$  [50] because they are softer than the neutral metallic atoms.

According to the frontier molecular orbital theory (FMO) of chemical reactivity, transition of electron is due to an interaction between HOMO and LUMO of reacting species. The energy of HOMO is directly related to the ionization potential and characterizes the susceptibility of the molecule toward attack by electrophiles. The energy of LUMO is directly related to the electron affinity and characterizes the susceptibility of the molecule toward attack by nucleophiles. Absolute hardness and softness are important properties to measure the molecular stability and reactivity. In the present study, TIPAS85 exhibits the lowest value of global hardness. It means that this one has a higher reactivity than CA92. Normally, the inhibitor with the least value of global hardness (hence the highest value of global softness) is expected to have the highest inhibition. The volume of molecule increases with the increase of dipole moment ( $\mu$ ), which increase the contact area between molecule and surface of iron and increases the corrosion inhibition. The global electrophilicity index, ( $\omega$ ) shows the ability of the inhibitor molecules to accept electrons. It is a measure of the stabilization in energy after a system accepts additional amount of electron charge  $\Delta N$  from the environment [48]. In our study, TIPAS85, with high electrophilicity index value than CA92, is the strongest nucleophile and therefore has the highest inhibition efficiency [51]. The calculated  $\Delta E_{back-donation}$  values for the inhibitors as listed in Table 9 reveal that the order followed is: TIPAS85 > CA92 which indicates that back-donation is favored for TIPAS85 which is the best inhibitor. According to nearly identical structure of TIPAS85 and CA92. The small differences between  $\Delta E$ ,  $\Delta N$ ,  $\eta$ ,  $\sigma$  can be supported by large difference between dipole moment and molecular dynamics results in that TIPAS85 has higher inhibition. TIPAS85 have larger steric hindrance because its structure that make it can let Cl<sup>-</sup>, oxygen and water little more far away from Fe than CA92.

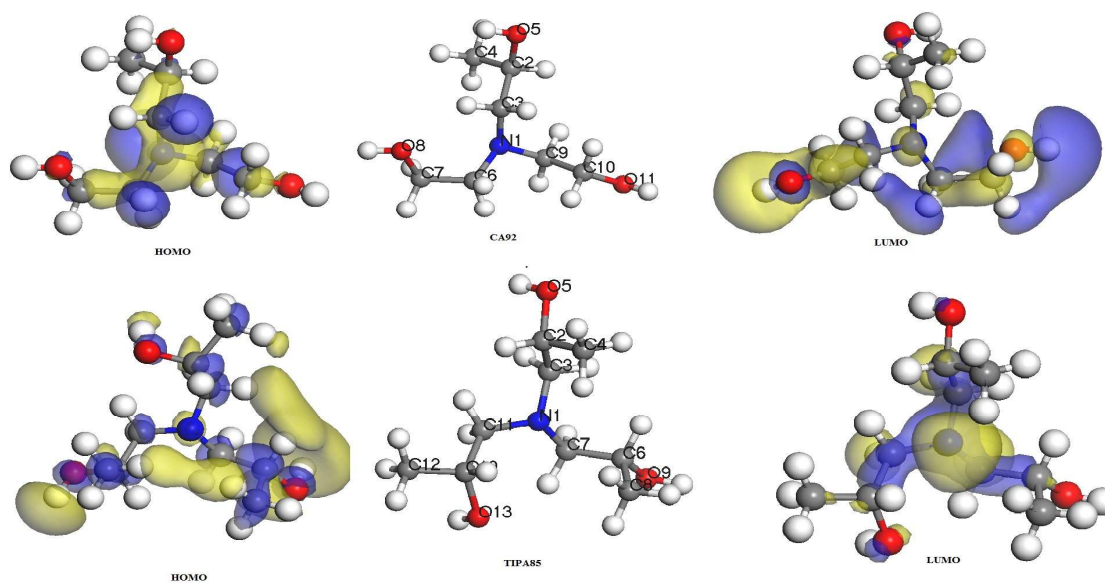


Fig.9: DMol<sup>3</sup> schematic representation of studied molecules

Table 9: Quantum-chemical descriptors for alcamines obtained with DFT method

Comp.,	Quantum-chemical descriptors												
	$I_p$ , eV	$E_A$ , eV	$\Delta E$ , eV	$\eta$ , eV	$\sigma$ , eV	CP, eV	X, eV	$\Delta N$	$\mu$ , D	$\omega$	$\Delta E_{back\ donation}$	S, Area	$E_{tot}$ , Ha
TIPA85	4.78	-1.11	5.89	2.95	0.34	-1.84	1.84	0.876	4.76	0.57	-0.74	829.14	-635.98
CA92	4.76	-1.22	5.97	2.99	0.34	-1.77	1.77	0.875	3.22	0.52	-0.75	748.21	-557.37

The effective atomic charges from Mulliken populations of the TIPA85 and CA92 in Table 10 shows that (N1, C4, O5, C8, O9, C12 and O13), (N1, O4, O7, C10 and O11) carry negative charges in TIPA85 and CA92 respectively. This indicated that these atoms are the negative charge centers that could offer electrons to the Fe atoms to form coordinate bond, and other carbon atoms are the positive charge centers that can accept electrons from 3d orbital of the Fe atoms to form feedback bond, thus further strengthening the interaction of inhibitor and Fe surface. Frontier orbital electron densities on atoms provide a useful means for the detailed characterization of donor-acceptor interactions. However, frontier electron densities can strictly be used only to describe the reactivity of different atoms in the same molecule [43]. To compare the reactivities of different molecules, frontier electron densities have to be normalized by the energy of the corresponding frontier molecular orbitals:  $F^E = f(r)/E_{HOMO}$ ,  $F^N = f(r)/E_{LUMO}$ . As shown in Table 10, the HOMO of TIPA85 is mainly constituted by N1 and the LUMO is constituted by O5, O9 and O13 which indicating that N1 can provide electrons and O5, O9 and O13 can accepting electrons. The HOMO of CA92 is mainly constituted by N1 and the LUMO is constituted by O4 and O7 which indicating that N1 can provide electrons and O4, O7 can accepting electrons

Table 10: The highest Fukui indices values by Hirshfeld methods and Mulliken charges for alcamines in liquid phase calculated with BOP / DNP basis set

Quantum-chemical descriptors																
TIPA 85	$f^+$	$f^-$	Mulliken	$F^N$	$F^E$	LUMO %	HOMO %	CA 92	$f^+$	$f^-$	Mulliken	$F^N$	$F^E$	LUMO %	HOMO %	
N1	0.01	0.23	-0.35	0.17	-1.32	2.28	48.54	N1	0.01	0.25	-0.37	0.18	-1.42	2.31	46.98	
C2	0.02	0.01	0.24	0.37	-0.07	4.89	2.72	C2	0.06	0.02	0.19	1.27	-0.13	16.43	4.34	
C3	0.01	0.04	0.00	0.32	-0.23	4.23	8.37	C3	0.02	0.04	0.07	0.51	-0.25	6.63	8.30	
C4	0.02	0.01	-0.20	0.56	-0.06	7.49	2.09	O4	0.11	0.03	-0.58	2.46	-0.18	31.70	6.04	
O5	0.04	0.03	-0.59	1.08	-0.18	14.33	6.49	C5	0.04	0.02	0.17	0.94	-0.10	12.10	3.21	
C6	0.02	0.01	0.22	0.54	-0.06	7.17	2.30	C6	0.02	0.05	0.01	0.36	-0.26	4.61	8.68	
C7	0.01	0.04	0.01	0.25	-0.23	3.26	8.37	O7	0.07	0.02	-0.57	1.59	-0.11	20.46	3.58	
C8	0.02	0.01	-0.20	0.56	-0.05	7.49	1.88	C8	0.01	0.02	0.25	0.11	-0.09	1.44	3.02	
O9	0.05	0.02	-0.57	1.15	-0.12	15.31	4.39	C9	0.01	0.04	0.01	0.20	-0.22	2.59	7.17	
C10	0.02	0.01	0.22	0.52	-0.06	6.84	2.30	C10	0.002	0.02	-0.19	0.04	-0.09	0.58	2.83	
C11	0.01	0.03	0.01	0.29	-0.17	3.91	6.28	O11	0.004	0.03	-0.58	0.09	-0.18	1.15	5.85	
C12	0.02	0.01	-0.20	0.54	-0.05	7.17	1.88									
O13	0.05	0.02	-0.57	1.18	-0.12	15.64	4.39		TIPA 85			$E_{HOMO}$ , Ha	$E_{LUMO}$ , Ha	CA 92	$E_{HOMO}$ , Ha	$E_{LUMO}$ , Ha
												-0.176	0.041		-0.175	0.045

## CONCLUSIONS

Two alcamines were tested as candidate inhibitors for reinforcement corrosion in aqueous solutions, cement grinding aids and cement quality improvement agent. Corrosion inhibitor can be used as interground additive in cement production to produce cement with more inhibiting character for steel corrosion by aggressive chloride ions. Ball milling creates fresh surfaces and these may be especially reactive. If the organic compounds bonds especially well to fresh surfaces this could affect reaction kinetics during subsequent hydration in a different way than if addition were to mix water. When lower concentrations of alcamines added to the cement ball mill. This leads to an increase in surface area of the constituent/cement, and accelerate cement hydration than cement hydration if alcamines add to cement as inhibitors admixtures. This also suggests that alcamines not only play as a grinding aid but also have a chemical role. This is an indication that the total number of moles of alcamines in the system is also an important factor.

Based on potentiodynamic curves and EIS curves, chemical and physical methods on cement, molecular dynamic simulation and quantum chemical studies the following conclusion can be drawn:

1. TIPA85 showed more inhibition than CA92. Both act as mixed -type inhibitor
2. The inhibition is due to adsorption of the alcamines molecules on the steel surface and blocking its active sites by its heteroatoms.
3. Adsorption of the investigated alcamines fits a Langmuir isotherm mode.
4. Alcamines suitable for using as grinding aids as indicated from cement fineness and strength improver for concrete and mortars.
5. Theoretical studies are consistent with experimental results.

## Acknowledgements

The authors thanks the Department of chemistry, Faculty of Science, El-Mansoura University and grateful for financial support from El Arish Cement Co., ArCC, Egypt.

## References

- 1 U. Mäder, Sheffield Academic Press, 1994, 2, 851
- 2 B. Anna, C. Tiziano, G. Mariagrazia and M. Matteo, Mapei S.p.A., via Cafiero 22, 20158 Milano, Italy.
- 3 L. Sottili, D. Padovani, and A. Bravo, *Cement Build Mater* 2002, 9, 40.
- 4 R.L. Camacho, E. Montiel, N. Jayanthi, T. Pandiyan and J. Cruz, *Chem. Phys. Letters*, 2010, 485, 142.
- 5 T. Arslan, F. Kandemirli, E.E. Ebenso, I. Love and H. Alemu, *Corros. Sci.*, 2009, 51, 35.
- 6 G. Gece, *Corros. Sci.*, 2008, 50, 2981.
- 7 K.F. Khaled, *Electrochim. Acta*, 2009, 54, 4345.
- 8 S. Ramachandran and V. Jovancevic, *Corrosion* 1999, 55, 259.
- 9 L. Li and A. A. Sagues, *Corrosion*, 2004, 60, 195.
- 10 M. F Hurley and J. R. Scully, *Corrosion*, 2006, 62, 892.
- 11 S.R. Allahkaram and M. Khodayari, *Anti-Corros. Methods Mater.*, 2008, 55, 250.
- 12 M. M. Mennucci, E. P. Banczek, P. R. P. Rodrigues and I. Costa, *Cement & Concrete Composites.*, 2009, 31, 418.
- 13 A.S. Fouda, Y.A. Elewady, H.K. Abd El-Aziz and A.M. Ahmed, *Int. J. Electrochem. Sci.*, 2012, 7, 10456.
- 14 A. Rashwani, Y. Alrakhban and A. Watti, *Arab. J. Chem.*, 2012, 5, 263.
- 15 S. Satoh, H. Fujimoto and H. Kobayashi, *J. Phys. Chem. B.*, 2006, 110, 4846.
- 16 S. Xia, M. Qiu, L. Yu, F. Liu and H. Zhao, *Corros. Sci.*, 2008, 50, 2021.
- 17 B. Delley, *J. Chem. Phys.*, 1990, 92, 508.
- 18 B. Delley, *J. Chem. Phys.*, 2000, 113, 7756.
- 19 R.S. Mulliken, *J. Chem. Phys.*, 1955, 23, 1833.
- 20 K.F. Khaled, *Electrochim. Acta*, 2003, 48, 2493.
- 21 X. Zhou, H. Y. Yang and F. H. Wang, *Electrochim. Acta*, 2011, 56, 4268.
- 22 C.N. Cao, *Chemical Industrial Engineering Press*, 2004, 325.
- 23 J. R. MacDonald, *Impedance Spectroscopy -Emphasizing Solid Materials and Systems*, John Wiley & Sons, New York, 1987.
- 24 J. Xu, L. Jiang, and J. Wang, *Constr. Build. Mater.*, 2009, 23, 1902.
- 25 C. Andrade, M. Keddad, X. R. Nóvoa, M. C. Pérez, C. M. Rangel, and H. Takenouti, *Electrochim. Acta*, 2001, 46, 3905.
- 26 W. Chen, R. G. Du, C. Q. Ye, Y. F. Zhu and C. J. Lin, *Electrochim. Acta*, 2010, 55, 5677.
- 27 Autolab Application Note COR04, 2011, 3.
- 28 E.H. El Ashry, A. El Nemr, S.A. Essawy and S. Ragab, *Prog. Org. Coat.*, 2008, 61, 11.
- 29 C.E. Ogukwe, C.O. Akalezi, M. A. Chidieber, K.L. Oguzle, Z.O. Iheabunike and E.E. Oguzle, *Portugal. Electrochim. Acta*, 2012, 30, 189.
- 30 C.N. Cao, *Chemical Industry Press*, 2004, 246.
- 31 X. Zhou, H. Y. Yang and F. H. Wang, *Acta Physico-Chimica Sinica*, 2011, 27, 647.
- 32 Y. Guo, X.P. Wang, Y.F. Zhu, J. Zhang, Y.B. Gao, Z.Y. Yang, R.G. Du and C.J. Lin, *Int. J. Electrochem. Sci.*, 2013, 8, 12769.
- 33 A. M. Fekry and M. A. Ameer, *Int. J. Hydrogen Energy*, 2010, 35, 7641.
- 34 A. M. Abdel-Gaber, E. Khamis and A. Hefnawy, *Mater. Corros.*, 2011, 62, 1159.
- 35 M. M. Page, C. L. Page, S. J. Shaw and S. Sawada, *J. Sep. Sci.*, 2005, 28, 471.
- 36 X. Zhou, H. Y. Yang and F. H. Wang, *Electrochim. Acta*, 2011, 56, 4268.
- 37 A.K. Singh and M.A. Quraishi, *Corros. Sci.*, 2010, 52, 1378.
- 38 M. Katsioti, P.E. Tsakiridis, P. Giannatos, Z. Tsibouki and J. Marinos, *Construct. Build. Mater.*, 2009, 23, 1954.
- 39 D. Bjegovic and V. Ukrainczyk, *NACE*, 1997, 183.
- 40 M. Magistri and P. D'Arcangelo, *MAPEI*, 2009, 102.
- 41 O. S. B. Al-Amoudi, W.A. Al-Kutti, S. Ahmad and M. Maslehuddin, *Cem. Concr. Composites*. 2009, 31, 672.
- 42 M. M. Kabanda, I. B. Obot and E. E. Ebenso, *Int. J. Electrochem. Sci.*, 2013, 8, 10839.
- 43 M. Karelson and V.S. Lobanov, *Chemical Reviews* 1996, 96, 1027.
- 44 R.G. Parr, D.A. Donnelly, M. Levy and M. Palke, *J. Chem. Phys.*, 1978, 68, 3801.
- 45 H. Wang; X. Wang; H. Wang; L. Wang and A. Liu, *J. Mol. Model.*, 2007, 13, 147.
- 46 R.G. Pearson, *Inorg. Chem.*, 1988, 27, 734.
- 47 T.Y. Soror and M.A. El-Ziady, *Mater. Chem. Phys.*, 2002, 77, 702.
- 48 R.G. Parr; L. Szentpaly and S. Liu, *J. Am. Chem. Soc.*, 1999, 121, 1922.
- 49 V. S. Sastri and J. R. Perumareddi, *Corros. Sci.*, 1997, 53, 617.
- 50 M. J. S. Deward and W. Thiel, *J. Am. Chem. Soc.*, 1977, 99, 4899.
- 51 P. Udhayakala, A. Maxwell Samuel, T. V. Rajendiranc and S. Gunasekarand, *J. Chem. Pharmac. Res.*, 2013, 5, 142153.